GREEN CONGLOMERATE AND INVESTIGATION USING AQUEOUS EXTRACTION FROM DATURA METAL LEAVES FOR CUPROUS OXIDE NANOPARTICLES

Kalathur Kumar[a], S. Arul[b]
a Department of Mechanical Engineering, Sri Chandrasekharendra Saraswathi Viswa Maha vidyalaya , Kanchipuram, India.
b Department of Mechanical Engineering, Annamacharya Institute of Technology and Sciences, Tirupathi, India.

Abstract:-The Cuprous Oxide (Cu_2O) nanoparticles were synthesized by green synthesis method using copper as precursor and Ammonium chloride with Lactobacillus bulgaricus as reducing agent in presence of Datura metal leaf extract as bio-surfactant in an aqueous medium. The bio synthesized nanoparticles were describe the distinctive natured by X-ray diffraction (XRD) and the pattern unveil face centered cubic structure. The size of Cu_2O nanoparticles were observed by scanning electron microscopy (SEM). The results indicate that the Cu_2O nanoparticles have high purity and the average particles size is 32 nm. The elemental anatomy of matals has been identified by Energy Dispersive X-Ray Analysis (EDX). Also conducting Inductive Couple Plasma (ICP) for its propensity to identify and quantify all elements with the exception of Argon

Keywords: **Cuprous-Oxide, Nano-particles, Bio synthesis, Coating,Characterization, Tribological properties**

Introduction

Nanotechnology involves the study of matter at atomic and supramolecular level [1, 2]. This field includes its great achievement in the field of biomedical and biotechnology [3]. Nano-particles are the small particle having size range of 1-100 nm (1 nm = 10-9 m) [4]. Due to large surface to volume ratio, nanoparticles react in different manner than that of large particles having same composition [5]. Among all types of NPs, metallic NPs are most promising as they exhibits remarkable antibacterial properties, due to this property metallic nanoparticles are now great area of research because bacteria are now developing resistance against antibiotics [6-8]. NPs exhibit different properties than that of bulk materials. Specific physical (surface area, colour, temperature etc.), chemical, magnetic and optical property make them good for different applications [9]. Nano-particles can be classified as metallic, non-metallic, semiconductor, carbon based and nanoparticles can also be defined on the basis of number of dimensions i.e. 1-D, 2-D and 3-D [10-12].

There are number of application of Nanotechnology in various areas such as surface coating, cosmetics, electronic circuits, packaging industries and biomedical [13]. Nanotechnology provides antimicrobial packaging material [14]. Nano-particles loaded with plasmid DNA could be used for gene delivery [15]. Bone healing can be achieved by using PLGA nanoparticles [16]. Diagnosis can be done by using techniques like optical imaging (OI), ultrasound imaging (UI) and magnetic resonance imaging (MRI) etc. [17, 18]. Magnetic and luminescent NPs are used in MRI and optical imaging respectively [19, 20]. Blood sugar can be checked by using nanobots [21]. Gold nanoparticles are used for detection of cancer [22]. Iron oxide nanoparticles are used for tissue repair [23, 24]. Additives containing nanoscale materials have long been used in the production of lacquers and paints, for example, Copper oxide as colouring pigments and synthetic amorphous silica to influence the fluidity of lacquer [25, 26]. In recent years modern techniques have been developed to visualize and scientifically describe nanoscale materials and structures [27, 28]. It is therefore now possible to tailor the manufacture and use of nanomaterials and nanostructures in the coating industry to the specific needs of the various applications [29, 30].

Nanomaterials consist of definable structural components with a size range of 1 - 100 nanometers ($1nm = 10^{-9}$ m) in at least one dimension (See also the Commission's recommendation of 18 Oct 2011 for the definition of Nanomaterials (2014/696/EU)) [31, 32]. Nano-particles are a subset of nanomaterials having the above size range in all three dimensions [33, 34]. Both natural and anthropogenic nanomaterials occur in the environment [35, 36].

Nanotechnology uses engineered Nano-materials Cuprous oxide is a two-dimensional crystal consisting of carbon atoms that has excellent mechanical, thermal, and tribological properties. Additionally, the Nano size with properties of larger surface areas and rich oxygen containing functional groups can enhance the adhesive between the fillers and the chains in the polymer matrix [9], which is beneficial for improving the thermo-stability and wear resistance of the polymer composite. Meanwhile, Cu_2O can form a self-lubrication transfer film on the contact interfaces during the friction process, which endows the grapheme / polymer composite with a low and stable friction coefficient and wear rate [10, 12]. Nevertheless, Cu_2O Nano-particles prepared in ambient atmospheric pressure without inert gas protection are prone to oxidation because the oxides of Cu are thermo dynamically more stable than pure Cu. In addition, without proper protection copper Nano-particles are found to aggregate rigorously. Starch was used to control the growth of Nano-particles and protect them to avoid oxidation and aggregation. The

main objectives of the study were the synthesis of Cu_2O nanoparticles by precipitation method and their characterization using X-ray diffraction (XRD), scanning electron microscopy (SEM) and Energy-dispersive X-ray Spectroscopy. (EDX).

Experimental

Cu_2O Nanoparticles were synthesized by precipitation method using different precursors as pasteurized milk curdled by adding a Lactobacillus bulgaricus, Ammonium chloride with post-heating in DATURA METEL Plant liquid (by crushed and sciage leaf). In the First step, 1000mL of Lactobacillus bulgaricus added with 100grams of Ammonium chloride to synthesis solution under continuous rapid stirring. Subsequently, the 250grams of melted copper is poured in a vessel, which is containing of both of above. The color of the solution turned to yellow ocher. After the completion of reaction, the copper was taken from the vessel and allowed to settle overnight and the supernatant solution was then discarded cautiously. In second step again melt the copper, which is separated from above first step, pour it in another vessel, which is containing Datura Metal Leaf liquid washed with de-ionized water and ethanol for three times to take out the excessive starch bound with the Nano-particles. Ocher color precipitates (Fig. 1) Obtained are dried at room temperature. After drying, Nano-particles were stored in glass vial for further analysis.

Fig.1: Cu2O Nano-particles synthesized through precipitation method

Results and Discussion

1. X-ray Diffraction Analysis (XRD):

Figure 1 shows the XRD pattern of Cu_2O nanoparticles sample, which clearly reveals the structure of crystalline. The peaks in this pattern are sharp and have no significant scattering background and all the peaks match well with standard data. Peaks were quite consistent with those of the standard JCPDS Card No. 04-0836 for the standard spectrum of the pure fcc (face centered cubic) metallic Cu. Besides the metallic Cu peaks, several other diffraction peaks appeared at 29.63°, 36.54°, 42.44°, 61.57°, 73.58° and 77.49° corresponding to (110), (111), (200), (220), (311) and (222) planes of cuprite, respectively, indicate the formation of cubic cop- per (I) oxide nanocrystals [17, 18]. The (111) peak at 36.526 (d = 0.2454) is the most strong peak of the pattern, and (110) peak at 29.661 (d = 0.3015) is the weakest in intensity. The XRD shows the final product is a pure Cu_2O sample.

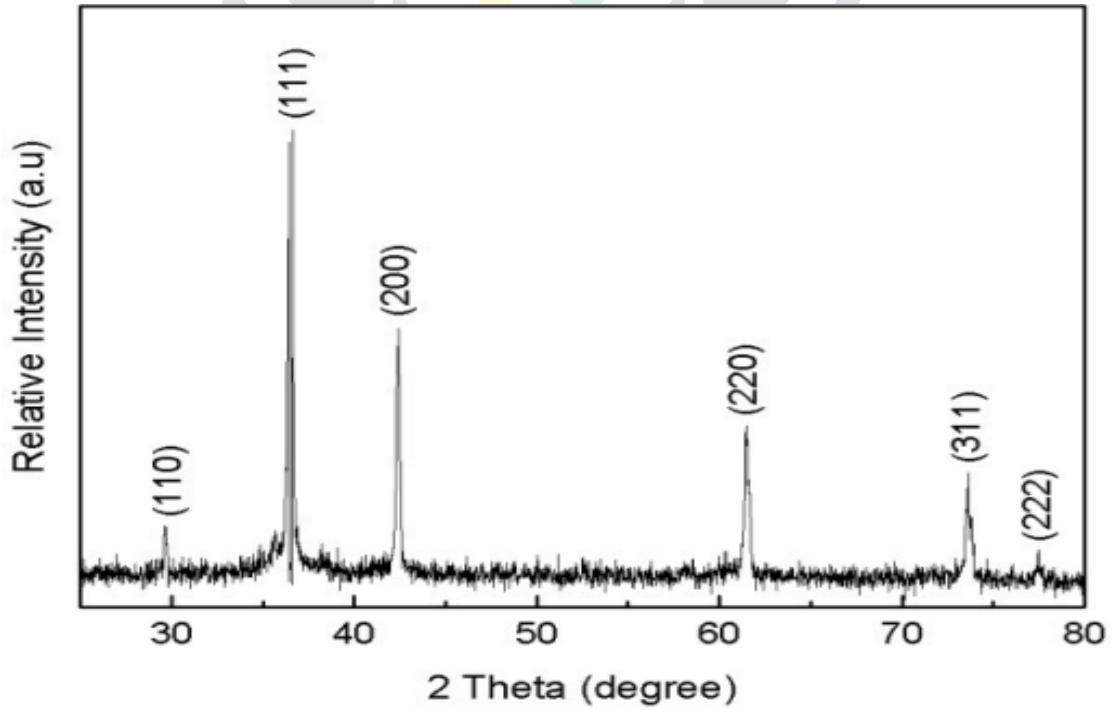

Fig.2: X-Ray Diffraction of Cu_2O nanoparticles

2. Scanning Electron Microscopy (SEM)

Scanning electron microscopy is used for inspecting topographies of specimens at very high magnifications using a piece of equipment called the scanning electron microscope. SEM magnifications can go to more than 300,000 X . SEM inspection is often used in the analysis of die/package cracks and fracture surfaces, bond failures, and physical defects on the die or package surface.

During SEM inspection, a beam of electrons is focused on a spot volume of the specimen, resulting in the transfer of energy to the spot. These bombarding electrons, also referred to as primary electrons, dislodge electrons from the specimen itself. The dislodged electrons, also known as secondary electrons, are attracted and collected by a positively biased grid or detector, and then translated into a signal.To produce the SEM image, the electron beam is swept across the area being inspected, producing many such signals. These signals are then amplified, analyzed, and translated into images of the topography being inspected. Finally, the image is shown on a CRT.

The ultimate resolution of the SEM depends primarily upon the tip size and shape. However, the solution resistance and mass and charge transfer process rates that affect the current density distribution are also important factors. Approximate expressions for the steady-state current that flows between substrate and tip as a function of z spacing for a conical and spherical tips in the generation/collection mode have been presented. The steady-state current mode would be of most interest for to photographic Information during x-y scans. The familiar plane/plane thin layer expression,

$$i = nFADC^*/d \qquad (1)$$

Where, d is the spacing between substrate and tip and
C* is the sum of the concentrations of oxidant,
C,, and of reductant, CR.
D is the diffusion coefficient (assuming Do = DR = D, in which DO and DR are the diffusion coefficients of oxidant (0) and reductant (R), respectively) and A is the electrode area.

An actual planar disk electrode will show behavior more like a hemispherical electrode, especially when d >> a (where a is the disk radius) under these conditions, or when the tip actually has a spherical or hemispherical shape, the approximate expression for i is

$$i = 2anFDC^*r \ln [1 + (r / d)] \qquad (2)$$

Where, (Y = a*/H, where a* is the cone base radius and H is the height) and y' = d/H. Thus a conical or tapered cylindrical tip would be less useful than an inlaid disk or hemisphere for probing the topography of a substrate. Actual tips may have more complex shapes as are sometimes observed in ultra microelectrodes. In the collection mode the tip is used as the detector only.

The usage of SEM to measure flow through membranes, investigate local transport properties and measure kinetic parameters of reactions. The impact of micro- electrochemical techniques on the understanding of physicochemical processes at interfaces, including transport across and within bilayers, monolayers, liquid /liquid interfaces and liquid / gas interfaces, has been a significant feature of this review. We have given several examples of using SEM to make per cellular measurements. There are clearly huge prospects for developing this avenue further, particularly for probing single cells, and improving spatial resolution of this type of measurement.

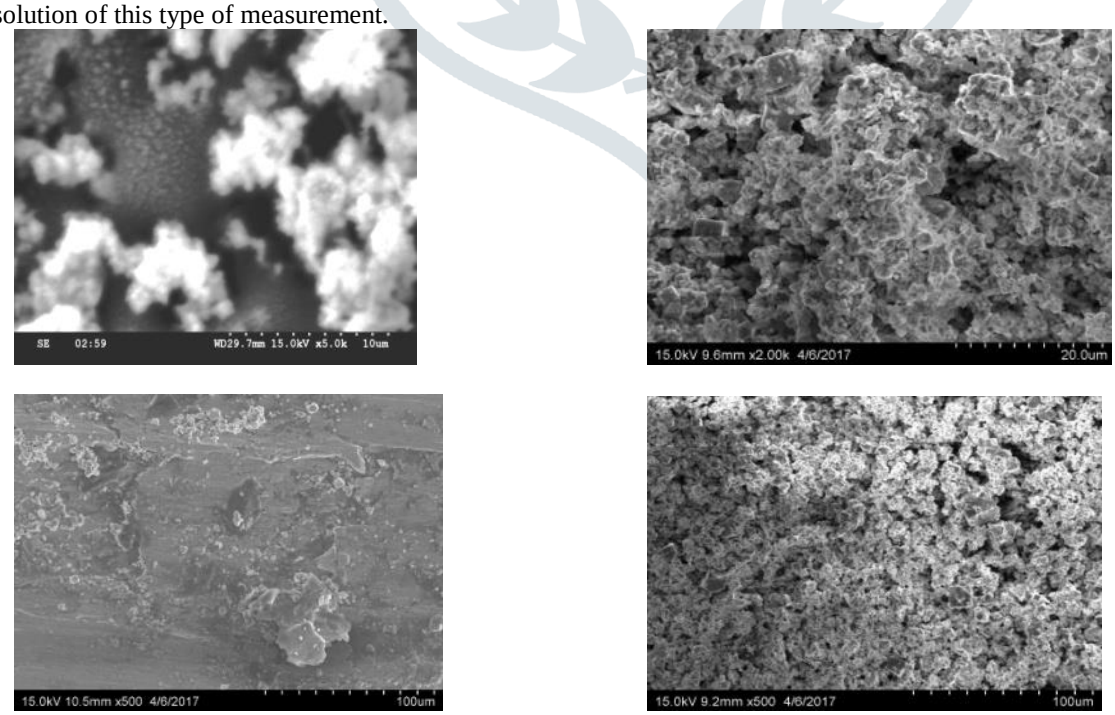

Fig.3: SEM Image

There is an impressive body of work on the use of microelectrodes to examine cellular processes at a single-cell level, such as exocytose, red-oxactivity and oxidative stress response. The application of mobile imaging probes, which are the distinguishing feature of SEM, should provide enhanced information on processes at single cells. Many recent technological developments in SEM have arrived from combining it with other physical techniques. However, the technique is in its infancy and much more work is necessary, notably the development of reliable methods for mass probe manufacture, to allow it to attain its full potential. Ring electrodes formed around optical fibers have been used to combine photo electrochemical microscopy (PEM).

3. Energy-Dispersive X-ray Spectroscopy (EDX):

EDX was carried out at an acceleration voltage of 20.0 kV. Sample was prepared by sprinkling the dispersed nanoparticles onto double-sided adhesive carbon conductive tape which was mounted on a microscopic stub of copper. From analyses results shown in the spectrographs in Figure 4, major constituent elements in the studied spectra were consistent with dominant elements showing closely related results with variation in the secondary and other elements recorded in smaller quantities represented by lower percentages. However, the differences between results could be seen as constituent elements minor variations and a test of purity and homogenous patterns of the organisms. Spectra indicated the dominance of carbon with mean value of 56.9 %, having 60.17 % peak and the lowest C content with 53.63 % in all the 4 spectra. Followed by oxygen with almost 9 % mean content having lowest O content of 7.02 % while highest was 8.37 %. Pt and Niobium(Nb) were 0.9 % while Mg was lowest in overall mean contents.

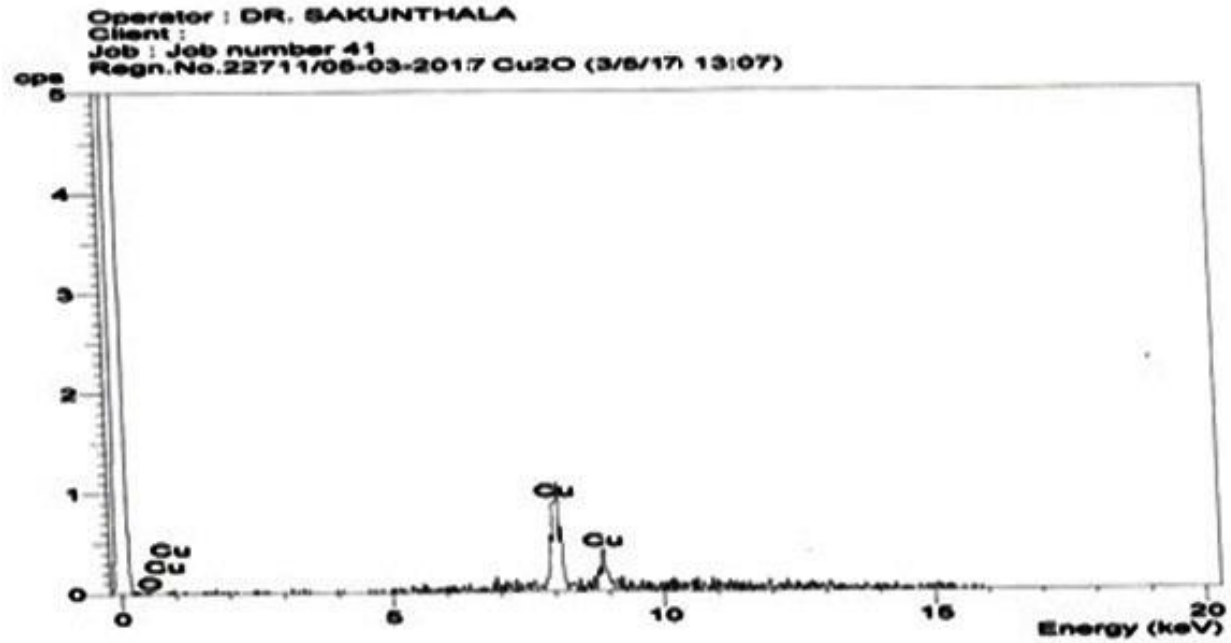

Fig 4. Energy-Dispersive X-ray

4. Inductive Couple Plasma (ICP):

Inductively coupled plasma mass spectrometry (ICPMS) for elemental analysis has been dominated since its introduction by instruments with quadrupole filters for mass separation. Although considerably impeded by isobaric ion interferences, ICPMS with quadrupoles has nevertheless matured to become the most prominent MS technique for element analysis with widespread applications, providing extremely low detection limits in combination with true multi element capabilities. Some years ago, a second generation of double-focusing ICPMS instruments was introduced, offering the chance to overcome interference problems by high mass resolution. The special features of these instruments for elemental analysis are discussed and the progress achieved in analytical performance is demonstrated by selected examples, emphasizing speciation as a field in which organic and inorganic aspects come close together.

Advantages of using an ICP include its ability to identify and quantify all elements with the exception of Argon; since many wavelengths of varied sensitivity are available for determination of any one element, the ICP is suitable for all concentrations from ultra trace levels to major components; detection limits are generally low for most elements with a typical range of 1 - 100 g / L. Probably the largest advantage of employing an ICP when performing quantitative analysis is the fact that multi elemental analysis can be accomplished, and quite rapidly. A complete multi element analysis can be undertaken in a period as short as 30 seconds,

consuming only 0.5 ml of sample solution. Although in theory, all elements except Argon can be determined using an ICP, certain unstable elements require special facilities for handling the radioactive fume of the plasma. Also, an ICP has difficulty handling halogens—special optics for the transmission of the very short wavelengths become necessary.

E-mail : test@mettexlab.com
Web : www.mettexlab.com
Phone : 044-22323163, 42179490, 91
Fax : 044-22311034

CHENNAI METTEX LAB PRIVATE LIMITED
Jothi Complex, 83, M.K.N. Road, Guindy, Chennai - 600 032.
ISO/IEC 17025 : 2005 NABL T436, T437, T1285

ISO/ IEC 17025 : 2005, ACCREDITATED BY NABL, DEPARTMENT OF SCIENCE AND TECHNOLOGY, GOVERNMENT OF INDIA

TEST REPORT

Page No. 1of 2

ISSUED TO : M/s. Kalathur Kumar.,
1-46, Marrimanda Village,
Yerpedu Mandal,
Chittoor - 517526

T.C Date : 20.09.2017
T.C No : CML/17-18/16712
Date Of Receipt : 14.09.2017
Completed On : 20.09.2017
Test Method : CML/W/SOP/52 (ICP)

Cust. Ref : Letter Dated : 14.09.17
Lab No : 1220027
Sample Description: 1 x 10 x 10 x 20 TATA Copper Powder.

S.NO	PARAMETERS	RESULTS
Platinum group metals		
01.	Palladium as Pd	BDL (DL : 0.05 mg/kg)
02.	Ruthenium as Ru	BDL (DL : 0.05 mg/kg)
03.	Iridium as Ir	BDL (DL : 0.05 mg/kg)
04.	Platinum as Pt	BDL (DL : 0.05 mg/kg)
05.	Osmium as Os	BDL (DL : 0.05 mg/kg)
06.	Rhodium as Rh	BDL (DL : 0.05 mg/kg)
Other Elements :-		
07.	Bismuth as Bi	2.76 mg/kg
08.	Gold as Au	BDL (DL : 0.03 mg/kg)
09.	Silver as Ag	6.80 mg/kg
10.	Lead as Pb	5.20 mg/kg
11.	Cadmium as Cd	22 mg/kg

.....Contd.....2

V.K. SELVAKUMAR
Authorized Signatory

Recognized / Approved by Airport Authority, Bureau of Indian Standards, Ministry of Environment & Forests, Rites & Defence

Note :- This report relates only to the particular sample submitted for test * Any correction not attested shall invalidate this report. This report shall not be reproduced except in full without our written approval. * Samples are not drawn by us unless otherwise stated. Retention period of tested samples one month only unless otherwise specified. # Indicates not come under the scope of accreditation.

CML / MSP / FRM / TRF-01

E-mail : test@mettexlab.com
Web : www.mettexlab.com
Phone : 044-22323163, 42179490, 91
Fax : 044-22311034

CHENNAI METTEX LAB PRIVATE LIMITED
Jothi Complex, 83, M.K.N. Road, Guindy, Chennai - 600 032.
ISO/IEC 17025 : 2005 NABL T436, T437, T1285

ISO/ IEC 17025 : 2005, ACCREDITATED BY NABL, DEPARTMENT OF SCIENCE AND TECHNOLOGY, GOVERNMENT OF INDIA

Continuation of T C No: CML/17-18/16712 Dated 20.09.2017

Page No. : 02 of 02

S.NO	PARAMETERS	RESULTS
12.	Nickel as Ni	BDL (DL : 0.05 mg/kg)
13.	Zinc as Zn	46.82 mg/kg
14.	Iron as Fe	175.2 mg/kg
15.	Arsenic as As	3.0 mg/kg
16.	Antimony as Sb	31 mg/kg
17.	Selenium as Se	22.0 mg/kg
18.	Tellurium as Te	47.0 mg/kg
19.	Copper as Cu	**93.10%**

Note: 1 mg/kg = 1 ppm
BDL: Below detection Limit, DL: Detection Limit

End of Report

For Chennai Mettex Lab Pvt Ltd.,

V.K. SELVAKUMAR
Authorized Signatory

Recognized / Approved by Airport Authority, Bureau of Indian Standards, Ministry of Environment & Forests, Rites & Defence

Note :- This report relates only to the particular sample submitted for test * Any correction not attested shall invalidate this report. This report shall not be reproduced except in full without our written approval. * Samples are not drawn by us unless otherwise stated. Retention period of tested samples one month only unless otherwise specified. # Indicates not come under the scope of accreditaion.

CML / MSP / FRM / TRF-01

Fig.5. Inductive Couple Plasma Testing

Conclusion

The study demonstrated a promising and generally applicable method to fabricate elemental copper nanoparticles by means of chemical reduction method. XRD results indicated that the starch-stabilized Cu2O nanoparticles are cubic in shape with mean size of 32 nm, respectively. Also we can find its ability to identify and quantify all elements with the exception of Argon by Inductive couple plasma (ICP). This synthesis pathway is particularly suitable for large-scale synthesis of Cu2O nanoparticles attributed to its simple process and low cost. It is probable that the development of improved synthetic methods for Cu2O nano crystals and more knowledge of their properties should lead to the great advancement in their applications such as catalysis and photo activated energy conversion.

References

1. Shenmar R, Norsten, V.B., Rotello, V.M.: Polymer-mediated nanoparticle assembly: structural control and applications. Adv. Mater. 6, 657–669 (2005)
2. Balzani, V., Credi, A., Venturi, M.: The bottom-up approach to molecular-level devices and machines. Chem. A Eur. J. 24, 5524–5532 (2002)
3. Lambert, S., Cellier, C., Gaigneaux, E.M., Pirard, J.P., Heinrichs, B.: Ag/SiO2, Cu/SiO2 and Pd/SiO2 cogelled xerogel catalysts for benzene combustion: relationships between operating synthesis variables and catalytic activity. Catal. Commun. 8, 1244–1248 (2007)
4. Zhang, H., Zhu, Q., Zhang, Y., Wang, Y., Zhao, L., Yu, B.: One- pot synthesis and hierarchical assembly of hollow Cu2O micro- spheres with nanocrystals-composed porous multishell and their gas-sensing properties. Adv. Funct. Mater. 17, 2766–2771 (2007)
5. Liu, Z., Bando, Y.: A novel method for preparing copper nanorods and nanowires. Adv. Mater. 15, 303–305 (2003)
6. Oritz, J.R., Ogura, T., Medina-Valtierra, J., Acosta-Ortiz, S.E., Bosh, P., De las Reyes, J.A., Lara, V.H.: A catalytic application of Cu2O and CuO films deposited over fiberglass. Appl. Surf. Sci. 174, 177–184 (2001)
7. Ke, H.; Huang, W.; Wang, X. Insights into the effect of thermocapillary migration of droplet on lubrication. Proc. Inst. Mech. Eng. Part J-J. Eng. Tribol. **2016**, 230, 583–590. [Google Scholar] [CrossRef]
8. Donnet, C.; Erdemir, A. Solid lubricant coatings: Recent developments and future trends. Tribol. Lett. **2004**, 17, 389–397. [Google Scholar] [CrossRef]
9. Zhang, D.-Y.; Zhang, P.-B.; Lin, P.; Dong, G.-N.; Zeng, Q.-F. Tribological properties of self-lubricating polymer-steel laminated composites. Tribol. Trans. **2013**, 56, 908–918. [Google Scholar] [CrossRef]
10. Katiyar, J.K.; Sinha, S.K.; Kumar, A. Friction and wear durability study of epoxy-based polymer (SU-8) composite coatings with talc and graphite as fillers. Wear **2016**, 362–363, 199–208. [Google Scholar] [CrossRef]
11. Wan, H.; Jia, Y.; Ye, Y.; Xu, H.; Cui, H.; Chen, L.; Zhou, H.; Chen, J. Tribological behavior of polyimide/epoxy resin-polytetrafluoroethylene bonded solid lubricant coatings filled with in situ-synthesized silver nanoparticles. Prog. Org. Coat. **2017**, 106, 111–118. [Google Scholar] [CrossRef]
12. Turssi, C.P.; Purquerio, B.M.; Serra, M.C. Wear of dental resin composites: Insights into underlying processes and assessment methods—A review. J. Biomed. Mater. Res. B **2003**, 65, 280–285. [Google Scholar] [CrossRef] [PubMed]
13. Bijwe, J.; Indumathi, J.; Ghosh, A.K. On the abrasive wear behaviour of fabric-reinforced polyetherimide composites. Wear **2002**, 253, 768–777. [Google Scholar] [CrossRef]
14. Bastani, D.; Esmaeili, N.; Asadollahi, M. Polymeric mixed matrix membranes containing zeolites as a filler for gas separation applications: A review. J. Ind. Eng. Chem. **2013**, 19, 375–393. [Google Scholar] [CrossRef]
15. Shen, X.-J.; Pei, X.-Q.; Fu, S.-Y.; Friedrich, K. Significantly modified tribological performance of epoxy nanocomposites at very low Cuprous oxide content. Polymer **2013**, 54, 1234–1242. [Google Scholar] [CrossRef]
16. Lin, J.; Wang, L.; Chen, G. Modification of Cuprous Oxide platelets and their tribological properties as a lubricant additive. Tribol. Lett. **2011**, 41, 209–215. [Google Scholar] [CrossRef]
17. Kandanur, S.S.; Rafiee, M.A.; Yavari, F.; Schrameyer, M.; Yu, Z.Z.; Blanchet, T.A.; Koratkar, N. Suppression of wear in Cu2O polymer composites. Carbon **2012**, 50, 3178–3183. [Google Scholar] [CrossRef]
18. Liu, D.; Zhao, W.S.; Liu, Q.; Cen, Q.; Xue, Q. Comparative tribological and corrosion resistance properties of epoxy composite coatings reinforced with functionalized fullerene C60 and Cu2O. Surf. Coat. Technol. **2016**, 286, 354–364. [Google Scholar] [CrossRef]
19. Liu, H.; Li, Y.; Wang, T.; Wang, Q. In situ synthesis and thermal, tribological properties of thermosetting polyimide/graphene oxide nanocomposites. J. Mater. Sci. **2012**, 47, 1867–1874. [Google Scholar] [CrossRef]
20. Ren, G.; Zhang, Z.; Zhu, X.; Ge, B.; Guo, F.; Men, X.; Liu, W. Influence of functional graphene as filler on the tribological behaviors of Nomex fabric/phenolic composite. Compos. Part A-Appl. Sci. Manuf. **2013**, 49, 157–164. [Google Scholar] [CrossRef]
21. Lahiri, D.; Hec, F.; Thiesse, M.; Durygin, A.; Zhang, C.; Agarwal, A. Nanotribological behavior of graphene nanoplatelet reinforced ultrahigh molecular weight polyethylene composites. Tribol. Int. **2014**, 70, 165–169. [Google Scholar] [CrossRef]
22. Muhammad, T.M.; Evie, L.P.; José, A.H.G.; Ilker, S.B.; Athanassi, A.; Luca, C. Graphene and polytetrafluoroethylene synergistically improve the tribological properties and adhesion of nylon 66 coatings. Carbon **2017**, 123, 26–33. [Google Scholar]
23. Shen, X.-J.; Pei, X.-Q.; Liu, Y.; Fu, S.-Y. Tribological performance of carbon nanotube–graphene oxide hybrid/epoxy composites. Compos. Part B-Eng. **2014**, 57, 120–125. [Google Scholar] [CrossRef]
24. Jiang, T.; Kuila, T.; Kim, N.H.; Ku, B.-C.; Lee, J.H. Enhanced mechanical properties of silanized silica nanoparticle attached graphene oxide/epoxy composites. Compos. Sci. Technol. **2013**, 79, 115–125. [Google Scholar] [CrossRef]
25. Golchin, A.; Wikner, A.; Emami, N. An investigation into tribological behaviour of multi-walled carbon nanotube/graphene oxide reinforced UHMWPE in water lubricated contacts. Tribol. Int. **2016**, 95, 156–161. [Google Scholar] [CrossRef]
26. Marcano, D.C.; Kosynkin, D.V.; Berlin, J.M.; Sinitskii, A.; Sun, Z.; Slesarev, A.; Alemany, L.B.; Lu, W.; Tour, J.M. Improved synthesis of graphene oxide. ACS Nano **2010**, 4, 4806–4814. [Google Scholar] [CrossRef] [PubMed]
27. ASTM E1461-01 Standard Test Method for Thermal Diffusivity by the Flash Method; ASTM International: West Conshohocken, CA, USA, 2001.

28. ASTM G133-05 Standard Test Method for Linearly Reciprocating Ball-on-flat Sliding Wear; ASTM International: West Conshohocken, CA, USA, 2005.
29. Zhang, D.; Dong, G.; Chen, Y.; Zeng, Q. Electrophoretic deposition of PTFE particles on porous anodic aluminum oxide film and its tribological properties. Appl. Surf. Sci. **2014**, 290, 466–474. [Google Scholar] [CrossRef]
30. Tai, Z.; Chen, Y.; An, Y.; Yan, X.; Xue, Q. Tribological behavior of UHMWPE reinforced with graphene oxide nanosheets. Tribol. Lett. **2012**, 46, 55–63. [Google Scholar] [CrossRef]
31. Naves, L.Z.; Santana, F.R.; Castro, C.G.; Valdivia, A.D.C.M.; da Mota, A.S.; Estrela, C.; Sobrinho, L.C.; Soares, C.J. Surface treatment of glass fiber and carbon fiber posts: SEM characterization. Microsc. Res. Tech. **2011**, 74, 1088–1092. [Google Scholar] [CrossRef] [PubMed]
32. Liu, L.H.; Yan, M. Functionalization of pristine graphene with perfluorophenyl azides. J. Mater. Chem. **2012**, 21, 3273–3276. [Google Scholar] [CrossRef]
33. Chatterjee, S.; Wang, J.W.; Kuo, W.S.; Tai, N.H.; Salzmann, C.; Li, W.L.; Hollertz, R.; Nüesch, F.A.; Chu, B.T.T. Mechanical reinforcement and thermal conductivity in expanded graphene nanoplatelets reinforced epoxy composites. Chem. Phys. Lett. **2012**, 531, 6–10. [Google Scholar] [CrossRef]
34. Lin, Z.; Mcnamara, A.; Liu, Y.; Moon, K.S.; Wong, C.P. Exfoliated hexagonal boron nitride-based polymer nanocomposite with enhanced thermal conductivity for electronic encapsulation. Compos. Sci. Technol. **2014**, 90, 123–128. [Google Scholar] [CrossRef]
35. Wang, F.; Drzal, L.T.; Qin, Y.; Huang, Z. Mechanical properties and thermal conductivity of graphene nanoplatelet/epoxy composites. J. Mater. Sci. **2015**, 50, 1082–1093. [Google Scholar] [CrossRef]
36. Ganguli, S.; Roy, A.K.; Anderson, D.P. Improved thermal conductivity for chemically functionalized exfoliated graphite/epoxy composites. Carbon **2008**, 46, 806–817. [Google Scholar] [CrossRef]
37. Pan, B.; Zhang, S.; Li, W.; Zhao, J.; Liu, J.; Zhang, Y.; Zhang, Y. Tribological and mechanical investigation of MC nylon reinforced by modified graphene oxide. Wear **2012**, 294–295, 395–401. [Google Scholar] [CrossRef]
38. Min, C.; Nie, P.; Song, H.J.; Zhang, Z.; Zhao, K. Study of tribological properties of polyimide/graphene oxide nanocomposite films under seawater-lubricated condition. Tribol. Int. **2014**, 80, 131–140. [Google Scholar] [CrossRef]
39. Feng, J.; Guo, Z. Temperature-frequency-dependent mechanical properties model of epoxy resin and its composites. Compos. Part B-Eng. **2016**, 85, 161–169. [Google Scholar] [CrossRef]